Prediction of Dispersivity for Undisturbed Soil Columns from Water Retention Parameters

E. Perfect,* M. C. Sukop, and G. R. Haszler

ABSTRACT

Dispersivity (α) is a required input parameter in solute-transport models based on the advection-dispersion equation (ADE). Normally α is obtained from miscible-displacement experiments. This dependency on inverse procedures imposes a severe limitation on our predictive capability. If solute breakthrough curves and soil hydraulic properties were measured simultaneously, pedotransfer functions could be developed to predict α from independent measurements. In this study, short (6 cm long) undisturbed columns were employed to investigate the relationship between α and the water-retention curve as parameterized by the air-entry value (ψ_a) and Campbell exponent (b). We worked with 69 columns from six soil types ranging in texture from loamy sand to silty clay, conventional-till and no-till management practices, steady-state saturated flow conditions, and a step decrease in $CaCl_2$ concentration from 0.009 to 0.001 M. Breakthrough curves were measured by monitoring changes in effluent electrical conductivity using a computerized data acquisition system. Estimates of α (calculated using the method of moments) ranged from 1 to 192 mm for the six soil types. Stepwise multiple-regression analysis explained ~50% of the total variation in α, and indicated that dispersion increased as ψ_a and b increased. Since both ψ_a and b increase with increasing clay content, α also increases moving from coarse- to fine-textured soils. Our regression equation can be used as a pedotransfer function to predict α from existing databases of soil hydraulic properties. Further research is needed to independently validate its predictive capability, and to develop strategies for upscaling the model predictions.

NUMEROUS MATHEMATICAL MODELS are available for describing solute transport in soil. Of these, the ADE is the most widely used. For steady state, one-dimensional water flow, the ADE for a nonreactive solute is given by (Fried and Combarnous, 1971):

$$\frac{\partial C}{\partial t} = \frac{\partial^2 C}{D \partial x^2} - v \frac{\partial C}{\partial x} \qquad [1]$$

where C is concentration of solute in the soil water (M L^{-3}), t is time (T), x is distance (L), D is the dispersion coefficient (L^2 T^{-1}), and v is the mean pore-water velocity (L T^{-1}). Equation [1] is normally applied to large volumes of homogeneous soil. Parker and van Genuchten (1984) have shown that, with appropriate boundary conditions, it is able to reproduce the highly asymmetric breakthrough curves obtained from short laboratory columns, even when continuous macropores are present. However, the use of Eq. [1] under such conditions remains a contentious issue (Germann, 1991; Feyen et al., 1998).

Because D in Eq. [1] depends upon v, it is desirable to define an alternative mixing parameter, the dispersivity $\alpha \equiv D/v$ (L), that can be related solely to characteristics of the porous medium (Fried and Combarnous, 1971). Dispersivity is a required input parameter in contaminant transport models based on the ADE (Zheng and Bennett, 1995). Except for a few simple systems such as packed beds of uniformly sized particles, α cannot be obtained from independent measurements (e.g., Koch and Flühler, 1993). Since most natural porous media are heterogeneous, soil physicists are currently unable to predict solute dispersion in undisturbed soil without first conducting a miscible-displacement experiment to measure it. This dependency on inverse procedures imposes a severe limitation on our predictive capability.

If solute breakthrough curves and static physical properties were determined on the same sample, empirical relations could be developed to predict α from independent measurements. However, such studies are remarkably rare, and most of them have used packed beds of disturbed media (Passioura and Rose, 1971; Han et al., 1985; Xu and Eckstein, 1997). Under saturated conditions, the magnitude of solute dispersion at any given flow rate is controlled by the pore-space geometry (Perfect and Sukop, 2001). Since it is the geometrical characteristics of solids or aggregates rather than the pore space that are measured in the packed bed approach, the resulting relationships are not directly applicable to undisturbed soil. While studies involving artificial macropores (Kanchanasut et al., 1978; Li and Ghodrati, 1997) may provide more information on the relationship between solute spreading and pore-space geometry, they are subject to similar criticisms regarding their applicability to natural systems.

In terms of heterogeneous systems, Anderson and Bouma (1977) observed greater Cl dispersion in undisturbed soil samples with subangular blocky structure as compared with those with prismatic structure. Walker and Trudgill (1983) reported significant correlations between solute transport parameters and several pore-geometry variables measured by image analysis of soil thin sections. Gist et al. (1990) showed that tracer dispersion in consolidated rocks was a function of the width of the pore-size distribution determined by Hg porosimetry. Network model simulations by Bruderer and Bernabé (2001) indicate that for a given flow rate, solute dispersion increases logarithmically as the normalized geometric standard deviation for a log-normal distribution of pores increases.

Several authors have investigated the relationship between pore structures revealed by dye-staining patterns and solute-transport parameters. Seyfried and Rao (1987) and Vervoort et al. (1999) report increasing solute dis-

E. Perfect, Dep. of Geological Sciences, Univ. of Tennessee, Knoxville, TN 37996; M.C. Sukop, Dep. of Plants, Soils and Biometeorology, Utah State Univ., Logan, UT 84322; G.R. Haszler, Dep. of Agronomy, Univ. of Kentucky, Lexington, KY 40546. Received 24 Apr. 2001. *Corresponding author (eperfect@utk.edu).

Table 1. Descriptions of the different soils and management treatments sampled.

Code	Soil	Classification	Mineralogy	Textural Class†	Management	No. of columns
A	Allegheny	Typic Hapludult	Mixed	Loam	Mixed grasses	6
B	Bruno	Typic Udifluvent	Mixed	Loamy sand	Mixed grasses	6
J	Jefferson	Typic Hapludult	Siliceous	Loam	Mixed grasses	6
K	Karnak	Vertic Endoaquept	Smectitic	Silty clay	Corn-soybean rotation	3
$M_{ct,0}$	Maury	Typic Paludalf	Mixed	Silt loam	Conventional-till corn (0 kg N ha^{-1})	9
$M_{ct,336}$	Maury	Typic Paludalf	Mixed	Silt loam	Conventional-till corn (336 kg N ha^{-1})	10
$M_{nt,0}$	Maury	Typic Paludalf	Mixed	Silt loam	No-till corn (0 kg N ha^{-1})	11
$M_{nt,336}$	Maury	Typic Paludalf	Mixed	Silt loam	No-till corn (336 kg N ha^{-1})	12
P	Pope	Fluventic Dystrudept	Mixed	Silt loam	Corn-soybean rotation	6

† Of A-horizon.

persivity with decreasing percentage of dyed area. The percentage of dyed area can be thought of as a flow weighted measure of pore size and connectivity, with small values corresponding to high macropore connectivity and vice versa. Hatano et al. (1992) investigated the relationship between solute dispersion and the fractal geometry of dye-staining patterns. These authors conducted Cl-miscible displacement experiments on undisturbed soil columns that were later destructively sampled, and their mass and surface fractal dimensions determined by image analysis of methylene blue dye stains. An empirical equation was obtained by regression analysis relating the dimensionless Brenner number (v multiplied by column length divided by D) for Cl breakthrough to both the mass and surface fractal dimensions of the dye-stained pore space.

Pore-space geometry also determines the retention and transport of water in soil. Since hydraulic properties such as the saturated hydraulic conductivity and parameters describing the water-retention curve are more frequently measured than pore characteristics, it seems logical to seek empirical relations between such properties and α. However, very few studies have explored this line of reasoning. Vervoort et al. (1999) investigated the relationship between α and soil hydraulic properties experimentally. They reported that α increased logarithmically as the reciprocal of the slope parameter from the water-retention curve increased. Computer simulations by Vogel (2000) suggest that different pore-size distributions can result in similar water-retention curves, and that solute dispersion is more sensitive to the water-retention curve than the pore-size distribution.

Databases of soil hydraulic properties are widely available (e.g., Rawls et al., 1991; Leij et al., 1996). Thus, if solute breakthrough curves and soil hydraulic properties were measured simultaneously on samples from a wide range of soil types, pedotransfer functions (Bouma, 1989) could be developed to predict α from information stored in existing databases. Pedotransfer functions are regression equations used to predict difficult-to-obtain parameters from more easily measured soil properties. They have been widely used to predict input parameters for soil hydrological models from basic soil properties such as particle-size distribution, bulk density, and organic C content (e.g., Rawls et al., 1991). To our knowledge however, this approach has not been previously applied to predict solute-transport parameters.

The major objectives of this study were: (i) to simultaneously measure solute-transport parameters and soil hydraulic properties on undisturbed columns from a wide range of soil types and management practices, and (ii) to establish an empirical relationship (pedotransfer function) between α and soil hydraulic properties. To facilitate these goals, we performed miscible-displacement experiments with a step change in electrolyte solution concentration under saturated, steady-state flow conditions, combined with measurements of total porosity, saturated hydraulic conductivity, and the soil water retention curve.

MATERIALS AND METHODS

Undistubed columns were obtained from the 2- to 8-cm depth of six different soil types with an Uhland sampler (Table 1). Sampling locations were selected on the basis of textural class and management history to give a wide range of soil hydraulic properties (Table 2). The Allegheny (fine-loamy, mixed, semiactive, mesic Typic Hapludults), Bruno (sandy, mixed, mesic Typic Udifluvents), Jefferson (fine-loamy, siliceous, semiactive, mesic Typic Hapludults), and Pope (coarse-loamy, mixed, active, mesic Fluventic Dystrudepts) soil columns were all obtained from the Robinson Agricultural Experiment Station, Quicksand, KY in May 1999. The Karnak (fine, smectitic, nonacid, mesic Vertic Endoaquepts) soil columns were collected from an agricultural field near Utica, KY in July 1998.

The Maury (fine, mixed, semiactive, mesic Typic Paleudalfs) soil columns came from long-term research plots at the University of Kentucky's Spindletop Agricultural Experiment Station, Lexington, KY. The treatments sampled were conventional-till and no-till corn (*Zea mays* L.), with ryegrass (*Secale cereale* L.) as a winter-cover crop, under two N fertilizer inputs (0 and 336 kg N ha^{-1}) (see Frye and Blevins, 1997 for details). Three subsamples were obtained from each of the four field replications. Sampling took place in May 1998, before tillage in the conventional-till treatment.

The 5.37-cm diam. by 6-cm long aluminum sleeves containing the soil columns were sealed in plastic bags, transported to the laboratory and stored at 4°C until required for analysis. Upon removal from storage, the columns were trimmed to remove any excess soil and were saturated from below with

Table 2. Mean soil hydraulic properties.†

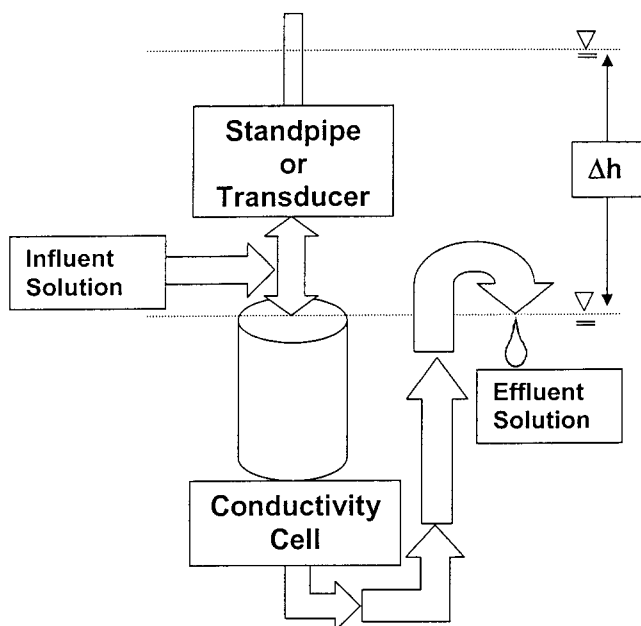| Code	ϕ	ψ_a	b	K_{sat}
	m^3 m^{-3}	kPa		10^{-6} m s^{-1}
A	0.44 (0.04)	3.0 (1.6)	4.9 (0.6)	1.7 (3.5)
B	0.59 (0.03)	2.6 (1.6)	2.5 (0.8)	12.4 (2.4)
J	0.48 (0.03)	13.2 (27.7)	5.1 (1.6)	6.1 (7.1)
K	0.49 (0.03)	34.5 (30.0)	6.4 (3.7)	0.7 (0.4)
$M_{ct,0}$	0.53 (0.07)	1.0 (0.5)	6.9 (2.0)	6.5 (6.2)
$M_{ct,336}$	0.56 (0.06)	0.7 (0.2)	6.5 (0.7)	9.1 (6.5)
$M_{nt,0}$	0.51 (0.04)	1.6 (1.0)	7.5 (1.3)	3.9 (3.3)
$M_{nt,336}$	0.61 (0.04)	0.7 (0.6)	6.7 (1.7)	15.1 (22.4)
P	0.54 (0.04)	8.8 (9.3)	4.8 (1.4)	1.6 (1.5)

† Mean value with standard deviation in parentheses.

Fig. 1. Schematic of the experimental set up for the miscible-displace-ment experiments; Δh is the hydraulic head.

Fig. 2. Representative solute breakthrough curves for Bruno loamy sand and Karnak silty clay.

a 0.009 M CaCl$_2$ solution. The ends of each column were covered with Nylon screens (Nitex 53-μm mesh, Sefar Amer-ica Inc., Briarcliff Manor, NY) and fitted into a plexiglass Tempe cell (Soilmoisture Equipment Corp., Santa Barbara, CA), with its porous ceramic base plate removed. The top inlet on the Tempe cell was connected to a precision peristaltic pump (Technicon AutoAnalyzer Proportioning Pump III, Technicon Corp., Tarrytown, NY). The bottom outlet on the Tempe cell was connected to a plexiglass conductivity cell, with electrodes formed by the faces of two stainless steel bolts. The conductivity cell was specially designed to minimize apparatus-induced dispersion relative to that produced by the soil columns.

The experimental setup for the miscible-displacement ex-periments is illustrated in Fig. 1. A steady flow of ~1.4 mL min^{-1} of 0.009 M CaCl$_2$ solution was pumped through the soil columns from top to bottom. A standpipe was connected to the inflow side of the Tempe cell to measure the head (Δh) developed across the column (Fig. 1). If the head exceeded that available in the laboratory, a pressure transducer (Tensimeter, Soil Measurement Systems, Tucson, AZ) was attached in place of the standpipe. Saturated conditions and a constant outflow head were maintained by piping the conductivity cell discharge back up to the top of the column (Fig. 1). The head was controlled at the outlet by a drip point. Assuming no head loss over the conductivity cell, the head loss over the sample is known and was used to determine the saturated hydraulic conductivity during the solute transport experiments.

After ~20 pore volumes, the concentration of the influent solution was changed to 0.001 M CaCl$_2$. When breakthrough was complete, the influent solution concentration was switched back to 0.009 M CaCl$_2$. These concentrations were selected to produce a mean ionic strength similar to field conditions (Seaman et al., 1995), and to maintain the structural integrity of the samples. Because of possible density-driven unstable mixing during a step increase in solute concentration with downward flow, only the step decrease was used to compute the breakthrough curve.

Four columns were run at a time, with the conductivity cells connected to a YSI Model 35 conductivity bridge (YSI Scientific, Yellow Springs, OH) via a multiplexer. The multi-plexer was controlled by a computer, and switched to each
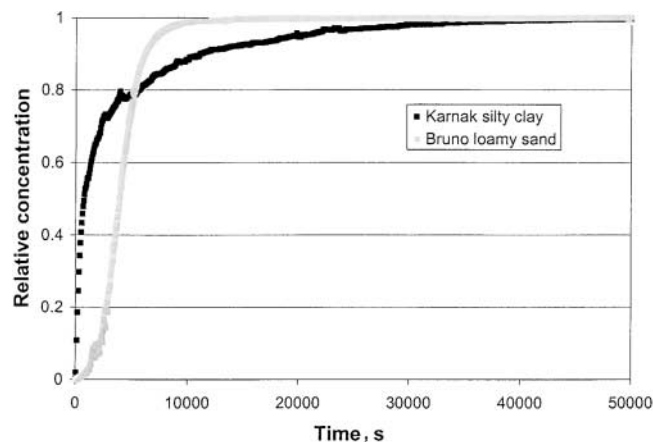
column once every minute. The voltage output of the conduc-tivity bridge (proportional to electrical conductivity) was simi-larly switched between one of four analog-digital conversion channels on a computer data acquisition board (CIO-DAS08/ Jr-AO, Computer Boards, Inc., Mansfield, MA). The analog input voltages were converted to digital values by the board. Data collection was managed using a program written with the LABTECH NOTEBOOK software package (LABTECH Corporation, Andover, MA). The outputs of this program consisted of ASCII files containing the voltage over time for each cell.

The voltage data were normalized to the voltage prior to the solution step change (taken as $C/C_0 = 0$) and to that after complete breakthrough was attained (taken as $C/C_0 = 1$). Typical breakthrough curves are shown in Fig. 2. The break-through curves were analyzed using the method of moments (Skopp, 1984; Jury and Sposito, 1985; Leij and Dane, 1991). The first, M_1 [T], and second, M_2 [T^2], central time moments for a step increase in solute concentration were computed using the trapezoidal rule (Yu et al., 1999). The ADE parame-ters, v and D, were estimated from M_1 and M_2 using the following expressions (Yu et al., 1999):

$$v = \frac{\ell}{M_1} \tag{2}$$

$$D = \frac{M_2 \ell^2}{2 M_1^3} \tag{3}$$

where ℓ is the length of the column [L]. By substituting Eq. [2] and [3] into our previous definition of dispersivity, an estimate of α is obtained.

Upon completion of the miscible-displacement experi-ments, a water-retention curve was determined for each col-umn. For the Maury and Karnak soils, the retention measure-ments were performed on the undisturbed columns using hanging water columns (Klute, 1986) over the tension range 0 to 5.0 $\times$ 10^0 kPa, and pressure plates (Klute, 1986) from 5.0 $\times$ 10^0 to 1.7 $\times$ 10^2 kPa. Pressure plates were used in conjunction with disturbed subsamples over the range 1.7 $\times$ 10^2 to 1.5 $\times$ 10^3 kPa (Klute, 1986). For the other soils, the undisturbed columns were employed down to a tension of 1.0 $\times$ 10^2 kPa using the same techniques as before. A dewpoint water activity meter (Gee et al., 1992) was then used in con-junction with disturbed subsamples to obtain the water-reten-tion curve from 1.0 $\times$ 10^2 to 4.8 $\times$ 10^5 kPa.

The water-retention curves were parameterized with the Campbell (1974) model:

$$S = \left(\frac{\psi}{\psi_a}\right)^{-\frac{1}{b}} \quad [4]$$

where S is relative saturation [$L^3 L^{-3}$] and ψ is the soil water tension [$M L^{-1} T^{-2}$]. This model has two fitting parameters: the air-entry value, ψ_a [$M L^{-1} T^{-2}$], which is inversely related to the size of the largest pores present, and the dimensionless constant, b, which is directly related to the width of the pore-size distribution. Equation [4] was fitted to the experimental data using segmented nonlinear regression analysis. The mean coefficient of determination (R^2) associated with these fits was >0.95. The resulting estimates of ψ_a and b, along with the total porosity (ϕ) and saturated hydraulic conductivity (K_{sat}), were used to characterize the hydraulic properties of each column.

RESULTS AND DISCUSSION

The textural classes of the six sampled soil types ranged from loamy sand to silty clay (Table 1). This relatively wide range in soil texture, coupled with the different management practices, produced a variety of pore structures and associated hydraulic properties (Table 2). Total porosity was the least variable property measured; there was no obvious relationship between the mean ϕ and soil texture (Table 2). In contrast, both ψ_a and b generally increased with increasing clay content (Table 2). The saturated hydraulic conductivity varied over three orders of magnitude, with values generally increasing with increasing porosity ($r = 0.41^{**}$).

The estimates of v and D for the different soils and management practices are summarized in Table 3. Because of the constant flow rate produced by the peristaltic pump, the v parameter exhibited relatively little variability, both between and within soil types. The smallest and largest values of D were obtained for the loamy sand and silty clay soils, respectively (Table 3). Within soil variability was extremely high for the D parameter, with coefficients of variation ranging from 30 to 700%.

The estimates of D generally increased as v increased (Fig. 3). Numerous authors have reported positive correlations between D and v. The most frequently encountered models are linear and power law relationships (Perfect and Sukop, 2001). Network simulations suggest a transition from Taylor dispersion ($D \propto v^2$) in homogenous porous media to mechanical dispersion ($D \propto v$) in heterogeneous porous media (Bruderer and Bernabé, 2001). In our study involving undisturbed soils, a linear model gave the best overall fit to the data (Fig. 3).

Following Elprince and Day (1977), we treated both v and D in Eq. [1] as adjustable parameters. This enabled us to evaluate any solute adsorption or exclusion effects without introducing an additional retardation factor. An effective transport porosity, ϕ_{eff} [$L^3 L^{-3}$], can be defined as (Elprince and Day, 1977):

$$\phi_{eff} = \frac{q}{v} \quad [5]$$

where q is the measured Darcy flux. Values of $\phi_{eff} < \phi$ denote solute exclusion, while values of $\phi_{eff} > \phi$ signify solute adsorption.

The mean values of ϕ_{eff} are given in Table 3. Comparison of the calculated ϕ_{eff} values in Table 3 with the corresponding measured values of ϕ in Table 2 suggests that effluent electrical conductivity was a conservative indicator of the water flux in most cases. For the Allegheny, Jefferson, and Pope soils however, $\phi_{eff} >> \phi$ indicating retardation of ions relative to the water flux. Cation adsorption in transport experiments is well documented (e.g., Schweich et al., 1983; Kool et al., 1989). Less well known is anion adsorption, which can occur in highly weathered acid soils such as Ultisols (Bellini et al., 1996; Korom, 2000). The Allegheny and Jefferson soils are both classified as Ultisols (see Table 1), and we speculate that they had appreciable anion as well as cation-exchange capacities which, combined with the low ionic strength of the solutions employed, served to retard the movement of both cations and anions. Seaman et al. (1995) observed a similar phenomenon with highly weathered, sandy aquifer material. Use of higher ionic strength solutions, much greater than would normally be encountered in the field, is recommended to eliminate this possibility in future laboratory studies.

The mean dispersivities ranged from <0.5 cm for Bruno loamy sand to >20 cm for Karnak silty clay (Table 3). Figure 4 shows the mean α values ranked from low to high, along with their corresponding textural classes. It can be seen that dispersivity generally increased sequentially moving from the coarser to finer textural classes.

Simple linear correlations between the solute-transport parameters and soil hydraulic properties are given in Table 4. The α was the most sensitive solute-transport parameter, producing significant correlations with three out of the four soil hydraulic properties investigated. The dispersivity increased as ϕ decreased, as ψ_a in-

Table 3. Mean solute transport parameters.†

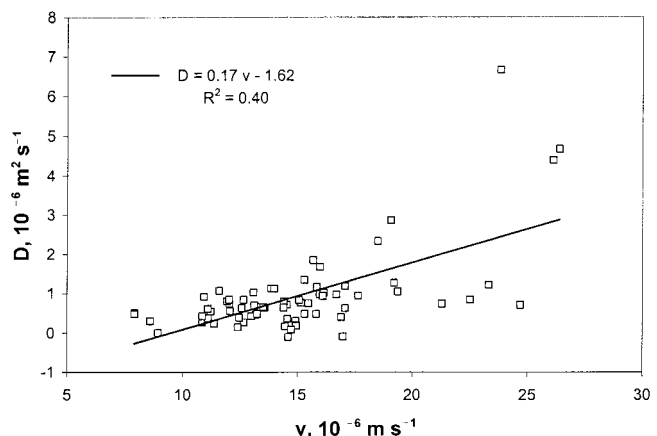| Code	v	D	α	ϕ_{eff}
	10^{-6} m s^{-1}	10^6 m^2 s^{-1}	10^{-3} m	m^3 m^{-3}
A	14.7 (1.9)	0.60 (0.19)	41 (34)	0.53 (0.12)
B	15.3 (1.1)	0.02 (0.14)	1 (9)	0.56 (0.03)
J	11.6 (3.4)	0.57 (0.29)	49 (19)	0.76 (0.16)
K	21.9 (5.6)	4.40 (2.42)	192 (82)	0.43 (0.13)
$M_{ct,0}$	15.6 (3.2)	0.80 (0.24)	51 (12)	0.59 (0.13)
$M_{ct,336}$	15.1 (4.8)	0.69 (0.34)	46 (20)	0.65 (0.23)
$M_{nt,0}$	16.3 (3.7)	1.23 (1.26)	67 (48)	0.56 (0.10)
$M_{nt,336}$	14.8 (4.1)	0.86 (0.64)	56 (35)	0.63 (0.15)
P	13.7 (2.3)	0.85 (0.30)	64 (25)	0.65 (0.10)

† Mean value with standard deviation in parentheses.

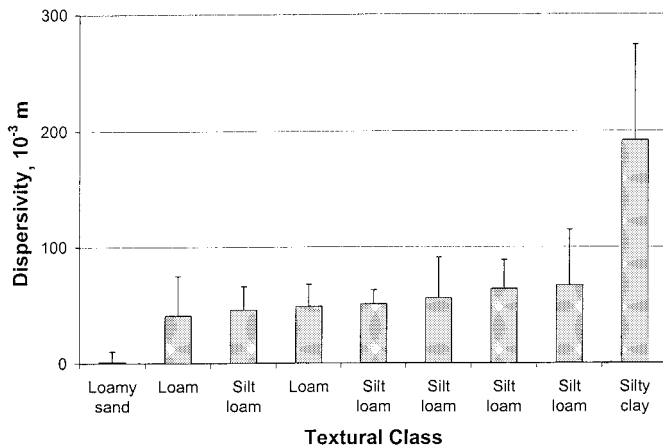Fig. 3. Relationship between D and v for the 69 soil columns.

Fig. 4. Ranked dispersivities and associated soil textural classes.

Fig. 5. Predicted, using the regression coefficients in Table 5, versus observed dispersivities.

creased, and as b increased (Table 4). The inverse relationship between ϕ and α is to be expected, since the tortuosity of connected flow paths increases as the porosity approaches the percolation threshold (Eggleston and Pierce, 1995). The positive relationship between α and ψ_a implies that fine-textured soils are more dispersive than coarse-textured soils. Similarly, the positive relationship between α and b means that dispersivity increases as the width of the pore-size distribution increases. A similar conclusion was reached by Vervoort et al. (1999).

The results of stepwise multiple-regression analyses relating the solute-transport parameters to soil hydraulic properties are summarized in Table 5. Once again dispersivity was the most sensitive parameter, with ψ_a and b combining to explain ~50% of the total variation in α (Table 5). Dispersivity increased as both ψ_a and b increased. Neither ϕ nor K_{sat} contributed significantly to the prediction of α once these two water-retention parameters were accounted for. Comparison of the observed and predicted dispersivities (Fig. 5) indicated the regression model tends to over-predict small values of α, and under-predict large values of α.

The fact that multiple-regression analysis could explain only half of the total variation in α may be related to the relatively narrow range of soil textures investi-
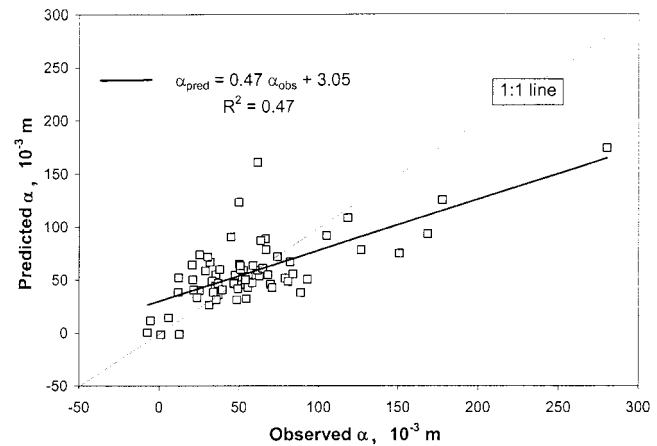
gated. Inclusion of additional data for sands and clays might improve the overall goodness of fit. Another source of unexplained variability is the different methods used to measure the water-retention curves for the different soils. It is also possible that the suite of predictor variables investigated (i.e., ϕ, ψ_a, b, and K_{sat}) did not provide a sufficiently complete or sensitive description of the actual pore-space geometry.

In an example application we used the regression coefficients in Table 5 as a pedotransfer function to predict $\alpha(\alpha_{pred})$ from the soil-water retention database of Cosby et al. (1984). These authors presented mean values of ψ_a and b for 11 soil textural classes ranging from sand to clay. Their data are reproduced in Table 6 along with our predicted dispersivities. All of the predictions were physically reasonable (i.e., no negative α values). Furthermore, there was a clear trend towards increasing dispersivity with increasing clay content. The range in α_{pred} for the 11 textural classes was 12 cm (Table 6). Given Fig. 5, this value is probably somewhat lower than the actual range in dispersivities that might be encountered.

A potential restriction on the use of our pedotransfer function is the dependence of α upon the measurement scale. Estimates of α tend to increase as the size of the solute transport experiment increases (Neuman, 1990; Gehlar et al., 1992). In this context, we note that all of the predictions in Table 6 are for 6-cm long columns.

Table 4. Correlations between solute transport parameters and soil hydraulic properties.†

Parameter	ϕ	ψ_a	b	K_{sat}
v	ns‡	ns	0.32 (0.0082)	ns
D	ns	0.40 (0.0008)	0.34 (0.0046)	ns
α	−0.31 (0.0098)	0.43 (0.0003)	0.36 (0.0026)	ns
ϕ_{eff}	ns	ns	ns	ns

† Pearson correlation coefficient with significance level in parentheses.
‡ Not significant at the 0.01 probability level.

Table 5. Results of stepwise-multiple regression analyses.

Parameter	Intercept	Variable 1	Variable 2	Model R^2
v, 10^{-6} m s^{-1}	11.27	b (0.62)†	ns‡	0.10
D, 10^{-6} m^2 s^{-1}	−1.01	ψ_a (0.05)§	b (0.29)	0.41
α, 10^{-3} m	−29.1	ψ_a (2.30)	b (12.7)	0.47
ϕ_{eff}	0.62	ns	ns	ns

† Variable selected with slope in parentheses.
‡ Not significant at the 0.01 probability level.
§ ψ_a in kPa.

Table 6. Dispersivity (predicted using the regression coefficients in Table 5) as a function of soil textural class.†

Textural Class	n	ψ_a	b	α_{pred}
		kPa		10^{-3} m
Sand	14	0.69	2.79	8
Loamy sand	30	0.36	4.26	26
Sandy loam	124	1.41	4.74	34
Loam	103	3.55	5.25	46
Silt loam	394	7.59	5.33	56
Sandy clay loam	104	1.35	6.77	60
Clay loam	147	2.63	8.17	81
Silty clay loam	324	6.17	8.72	96
Sandy clay	16	0.98	10.73	109
Silty clay	43	3.24	10.39	110
Clay	148	4.68	11.55	128

† Mean values of ψ_a and b from Cosby et al. (1984).

Further research is needed to develop appropriate strategies for upscaling these values to larger soil volumes.

CONCLUSIONS

We have developed a pedotransfer function for predicting the dispersivity of 6-cm long soil columns from the Campbell (1974) water-retention parameters: ψ_a and b. The model explained ~50% of the observed variability in α. Our analysis suggests that α increases as ψ_a and b increase. Since both ψ_a and b increase with increasing clay content, α also increases moving from coarse- to fine-textured soils. In an example application, we used the pedotransfer function to predict α for the 11 textural classes in the soil water-retention database of Cosby et al. (1984). The predictions ranged from 0.8 cm for sands to 12.8 cm for clays. The actual range in α at this scale is likely to be somewhat wider. Research is currently underway on refining and independently validating this pedotransfer function. We are also developing strategies for upscaling the model predictions.

REFERENCES

Anderson, J.L., and J. Bouma. 1977. Water movement through pedal soils. I saturated flow. Soil Sci. Soc. Am. J. 41:413–418.

Bellini, G., M.E. Sumner, D.E. Radcliffe, and N.P. Qafoku. 1996. Anion transport through columns of highly weathered acid soil: Adsorption and retardation. Soil Sci. Soc. Am. J. 60:132–137.

Bouma, J. 1989. Using soil survey data for quantitative land evaluation. Adv. Soil Sci. 9:177–213.

Bruderer, C., and Y. Bernabé. 2001. Network modeling of dispersion: Transition from Taylor dispersion in homogeneous networks to mechanical dispersion in very heterogeneous ones. Water Resour. Res. 37:897–908.

Campbell, G.S. 1974. A simple method for determining unsaturated conductivity from moisture retention data. Soil Sci. 117:311–314.

Cosby, B.J., G.M. Hornberger, R.B. Clapp, and T.R. Ginn. 1984. A statistical exploration of the relationships of soil moisture characteristics to the physical properties of soils. Water Resour. Res. 20:682–690.

Eggleston, J.R., and J.J. Peirce. 1995. Dynamic programming analysis of pore space. Eur. J. Soil Sci. 46:581–590.

Elprince, A.M., and P.R. Day. 1977. Fitting solute breakthrough equations to data using two adjustable parameters. Soil Sci. Soc. Am. J. 41:39–41.

Feyen, J., D. Jacques, A. Timmerman, and J. Vanderborght. 1998. Modelling water flow and solute transport in heterogeneous soils: A review of recent approaches. J. Agric. Eng. Res. 70:231–256.

Fried, J.J., and M.A. Combarnous. 1971. Dispersion in porous media. Adv. Hydroscience 7:169–282.

Frye, W.W., and R.L. Blevins. 1997. Soil organic matter under long-term no-tillage and conventional tillage corn production in Kentucky. p. 227–234. In E.A. Paul et al. (ed.) Soil organic matter in temperate agroecosystems: Long-term experiments in North America. CRC Press, Boca Raton, FL.

Gee, G.W., M.D. Campbell, G.S. Campbell, and J.H. Campbell. 1992. Rapid measurement of low water potentials using a water activity meter. Soil Sci. 56:1068–1070.

Gelhar, L.W., C. Welty, and K.R. Rehfeldt. 1992. A critical review of data on field-scale dispersion in aquifers. Water Resour. Res. 28:1955–1974.

Germann, P.F. 1991. Length scales of convection-dispersion approaches to flow and transport in porous media. J. Contam. Hydrol. 7:39–49.

Gist, G.A., A.H. Thompson, A.J. Katz, and R.L. Higgins. 1990. Hydrodynamic dispersion and pore geometry in consolidated rock. Phys. Fluids A 2:1533–1544.

Han, N., J. Bhakta, and R.G. Carbonell. 1985. Longitudinal and lateral dispersion in packed beds: Effect of column length and particle size distribution. AIChE. J. 31:277–288.

Hatano, R., N. Kawamura, J. Ikeda, and T. Sakuma. 1992. Evaluation of the effect of morphological features of flow paths on solute transport by using fractal dimensions of methylene blue staining pattern. Geoderma 53:31–44.

Jury, W.A., and G. Sposito. 1985. Field calibration and validation of solute transport models for the unsaturated zone. Soil Sci. Soc. Am. J. 49:1331–1341.

Kanchanasut, P., D.R. Scotter, and R.W. Tillman. 1978. Preferential solute movement through larger soil voids. II. Experiments with saturated soil. Aust. J. Soil Res. 16:269–276.

Klute, A. 1986. Water retention: Laboratory methods. p. 635–662. In A. Klute (ed.) Methods of soil analysis. Part 1. 2nd ed. Agron. Monogr. 9. ASA and SSSA, Madison, WI.

Koch, S., and H. Flühler. 1993. Solute transport in aggregated porous media: comparing model independent and dependent parameter estimation. Water Air Soil Pollut. 68:275–289.

Kool, J.B., J.C. Parker, and L.W. Zelazny. 1989. On the estimation of cation exchange parameters from column displacement experiments. Soil Sci. Soc. Am. J. 53:1347–1355.

Korom, S.F. 2000. An adsorption isotherm for bromide. Water Resour. Res. 36:1969–1974.

Leij, F.J., W.J. Alves, M.Th. van Genuchten, and J.R. Williams. 1996. Unsaturated soil hydraulic database, UNSODA 1.0 User's manual. Rep. EPA/600/R-96/095, US EPA, Ada, OK.

Leij, F.J., and J.H. Dane. 1991. Solute transport in a two-layer medium investigated with time moments. Soil Sci. Soc. Am. J. 55:1529–1535.

Li, Y., and M. Ghodrati. 1997. Preferential transport of solute through soil columns containing constructed macropores. Soil Sci. Soc. Am. J. 61:1308–1317.

Neuman, S.P. 1990. Universal scaling of hydraulic conductivities and dispersivities in geologic media. Water Resour. Res. 26:1749–1758.

Parker, J.C., and M.Th. van Genuchten. 1984. Determining transport parameters from laboratory and field tracer experiments. Virginia Agric. Exp. Stn. Bull. 84-3, Virginia Polytechnic Inst. and State Univ., Blacksburg, VA.

Passioura, J.B., and D.A. Rose. 1971. Hydrodynamic dispersion in aggregated media 2. Effects of velocity and aggregate size. Soil Sci. 111:345–351.

Perfect, E., and M.C. Sukop. 2001. Models relating solute dispersion to pore space geometry in saturated media: A review. p. 77–146. In H.M. Selim and D.L. Sparks (ed.) Physical and chemical processes of water and solute transport/retention in soils. SSSA Special Publ. 56. SSSA, Madison WI.

Rawls, W.J., T.J. Gish, and D.L. Brakensiek. 1991. Estimating soil water retention from soil physical properties and characteristics. Adv. Agron. 16:213–234.

Schweich, D., M. Sardin, and J.-P. Gaudet. 1983. Measurement of a cation exchange isotherm from elution curves obtained in a soil column: Preliminary results. Soil Sci. Soc. Am. J. 47:32–37.

Seaman, J.C., P.M. Bertsch, and W.P. Miller. 1995. Ionic tracer movement through highly weathered sediments. J. Contam. Hydrol. 20: 127–143.

Seyfried, M.S., and P.S.C. Rao. 1987. Solute transport in undisturbed columns of an aggregated tropical soil: Preferential flow effects. Soil Sci. Soc. Am. J. 51:1434–1444.

Skopp, J. 1984. Analysis of solute movement in structured soils. p. 220–227. In J. Bouma and P.A.C. Raats (ed.) Proc. ISSS Symp. Water and solute movement in heavy clay soils. ILRI, Wageningen, the Netherlands.

Vervoort, R.W., D.E. Radcliffe, and L.T. West. 1999. Soil structure development and preferential solute flow. Water Resour. Res. 35: 913–928.

Vogel, H.J. 2000. A numerical experiment on pore size, pore connectivity, water retention, permeability, and solute transport using network models. Eur. J. Soil Sci. 51:99–105.

Walker, P.J.C., and S.T. Trudgill. 1983. Quantimet image analysis of soil pore geometry: comparison with tracer breakthrough curves. Earth Surf. Processes Landforms 8:465–472.

Xu, M., and Y. Eckstein. 1997. Statistical analysis of the relationships between dispersivity and other physical properties of porous media. Hydrogeology J. 5:4–20.

Yu, C., A.W. Warrick, and M.H. Conklin. 1999. A moment method for analyzing breakthrough curves of step inputs. Water Resour. Res. 35:3567–3572.

Zheng, C., and G.D. Bennett. 1995. Applied contaminant transport modeling. Van Nostrand Reinhold, New York.